

Kinetic study of carbon nanotube synthesis over Mo/Co/MgO catalysts

著者	Ni Lei, Kuroda Keiji, Zhou Ling-Ping, Kizuka Tokushi, Ohta Keishin, Matsuishi Kiyoto, Nakamura Junji
journal or publication title	Carbon
volume	44
number	11
page range	2265-2272
year	2006-09
権利	(C) 2006 Elsevier Ltd.
URL	http://hdl.handle.net/2241/104137

doi: 10.1016/j.carbon.2006.02.031

Kinetic study of carbon nanotube synthesis over Mo/Co/MgO catalysts

Lei Ni^a, Keiji Kuroda^a, Ling-Ping Zhou^b, Tokushi Kizuka^a, Keishin Ohta^c,

Kiyoto Matsuishi^a, Junji Nakamura^{a, *}

^a *Graduate School of Pure and Applied Sciences, University of Tsukuba, Tennoudai 1-1-1, Tsukuba, Ibaraki 305-8537, Japan*

^b *The Research Institute of Petroleum Processing, Xueyuan Road 18, Beijing 100083, P. R. China*

^c *Microphase. co. Ltd., Toukoudai 5-9-1, Tsukuba, Ibaraki 300-2635, Japan*

Abstract

The kinetics of carbon nanotube (CNT) synthesis by decomposition of CH_4 over Mo/Co/MgO and Co/MgO catalysts was studied to clarify the role of catalyst component. In the absence of the Mo component, Co/MgO catalysts are active in the synthesis of thick CNT (outer diameter of 7-27 nm) at lower reaction temperatures, 823-923 K, but no CNTs of thin outer diameter are produced. Co/MgO catalysts are significantly deactivated by carbon deposition at temperatures above 923 K. For Mo-including catalysts (Mo/Co/MgO), thin CNT (2-5 walls) formation starts at above 1000 K without deactivation. The significant effects of the addition of Mo are ascribed to the reduction in catalytic activity for dissociation of CH_4 , as well as to the formation of Mo_2C during CNT synthesis at high temperatures. On both Co/MgO and Mo/Co/MgO catalysts, the rate of CNT synthesis is proportional to the CH_4 pressure, indicating that the dissociation of CH_4 is the rate-determining step for a catalyst working without deactivation. The deactivation of catalysts by carbon deposition takes place kinetically when the formation rate of the graphene network is smaller than the carbon deposition rate by decomposition of CH_4 .

Keywords: Carbon nanotube, Catalyst, Electron microscopy, Catalytic properties.

1. Introduction

Much research of carbon nanotube (CNT) has been carried out in respect to the growth mechanism, structure, morphology, and application of CNT because of their unique chemical and physical properties. Arc-vaporization [1, 2], laser ablation [3], and thermal chemical vapor deposition (CVD) [4] methods have been used for the synthesis of CNT. Catalytic chemical vapor deposition (CCVD) with its low cost and high yield, has been recognized as the most practical among all the CNT synthetic methods [5, 6]. The morphology and the quality of CNT depend on the catalysts, carbon sources, temperatures, flow rates and feedstock pressures. The effective catalysts for the CCVD growth of CNT are known to be Fe, Co and Ni. It is also known that the addition of Mo into Fe [7], Co [8, 9, 10], and Ni [11] catalysts leads to the formation of thin CNT. Hu et al. [9] have reported that Co-Mo catalysts show high selectivity and activity for the synthesis of single-walled carbon nanotube (SWNT) from ethanol, in which the role of Mo is considered to disperse Co molybdates and metallic Co. Herrela et al. [10] have also reported the formation of small Co clusters active for SWNT synthesis in Co-Mo/SiO₂ catalysts, where the formation of molybdenum carbide is observed.

In a study of the Ni/Mo/MgO catalyst [11], it has been found that the formation of molybdenum carbide is crucial for controlling the catalytic properties, because molybdenum is present as molybdenum carbide in a steady state of CNT synthesis at temperatures above 1000 K. On the other hand, the carbides of Ni, Co, and Fe are unstable at 1000 K. It has been suggested that the Mo component plays a role in reserving carbon in the bulk. That is, the presence of molybdenum carbide alters the kinetics of carbon migration into the bulk of the catalyst, and affects the segregation to the surface.

To clarify the role of the catalyst components, kinetic information is necessary concerning the constituent reactions steps such as dissociation of CH₄, the migration of carbon into the bulk of catalyst, segregation of carbon to the surface, and the formation of graphene networks. The kinetic balance will control the apparent catalytic activity and the catalyst deactivation for synthesis of

CNT. In this study, we carry out kinetic measurements such as pressure dependence and temperature dependence of CNT synthesis on Co/MgO and Mo/Co/MgO catalysts. The results are used to discuss the rate-determining step, the reason for the catalyst deactivation, and the role of the Mo component.

2. Experimental

2.1 Catalysts preparation

To prepare Mo/Co/MgO catalysts, $(\text{NH}_4)_6\text{Mo}_7\text{O}_{24} \cdot 4\text{H}_2\text{O}$, $\text{Co}(\text{NO}_3)_2 \cdot 6\text{H}_2\text{O}$ and $\text{Mg}(\text{NO}_3)_2 \cdot 6\text{H}_2\text{O}$ (Wako Pure Chemical Industries, Ltd., Osaka, Japan) were mixed stoichiometrically, ground thoroughly, and then followed by the addition of 1.2 g citric acid and several drops of de-ionized water. The mixture was ground again to make a uniform paste-like sample and calcined at 823 K in air for 20 min. The foam material obtained was used for CNT synthesis. Various catalysts with different compositions of Mo/Co/MgO and Co/MgO were thus prepared, where the composition was expressed by molar ratio; for example, $\text{Mo}_{0.1}\text{Co}_{0.4}\text{Mg}_{0.5}\text{O}$.

2.2 CNT synthesis

CNT was synthesized by the catalytic decomposition of methane diluted with nitrogen (1, 3, 5, and 10.4 % CH_4) at 773-1073 K over Mo/Co/MgO catalysts. Decomposition of methane was carried out in a fixed bed flow reactor made of quartz tube (i.d. 2.5 cm, length: 55 cm), laid on a horizontal furnace with a thermocouple in its central zone. Two quartz boats with 20 mg catalyst were placed in the central part of the reactor. The catalyst was heated to 923 K in N_2 (100 sccm) and then reduced for 1 h at 923 K with H_2 gas ($\text{H}_2/\text{N}_2 = 60/100$, v/v). Subsequently, the temperature was raised to the reaction temperature and methane (100 sccm) was fed in when the reaction temperature was stable. After the reaction, methane was switched to nitrogen (100 sccm) during cooling. The CNT with catalysts were finally collected from these two quartz boats. The carbon yield of each boat was calculated as follows:

$$\text{Carbon yield} = \frac{W_{\text{products}} - W_{\text{catalysts}}}{W_{\text{catalysts}}} \times 100\%,$$

where W_{products} and $W_{\text{catalysts}}$ denote the total weight of carbon and catalyst after the reaction, and the weight of catalyst before the reaction, respectively.

2.3 TEM and XRD

Transmission electron microscopy (TEM) observations were carried out using a JEOL JEM-2010FE TEM. X-Ray diffraction (XRD) measurements were carried out with an X'Pert MRD (Philips) diffractometer using nickel-filtered Cu K_{α} radiation. CNT samples were pressed on a Si single crystal plate. The patterns were recorded over $5^{\circ} < 2\theta < 90^{\circ}$.

3. Results and discussion

3.1 Effect of Mo on catalytic activity

CNT synthesis was carried out by decomposition of CH_4 (7.5-78 Torr) at 773-1073 K over Mo/Co/MgO and Co/MgO catalysts. While it is difficult to accurately determine the selectivity of CNT formation, TEM images of the products showed that CNT was formed with selectivity of over 90 % on Mo/Co/MgO and Co/MgO catalysts. Figures 1 (a) and (b) show TEM images of CNT formed at 1073 K by a $\text{Mo}_{0.025}\text{Co}_{0.05}\text{Mg}_{0.925}\text{O}$ catalyst (Mo:Co=1:2). Thin CNTs 3-10 nm in outer diameter were observed. The results are similar to those reported for Mo/Ni/MgO catalysts, where the outer diameter was equal to the diameter of the catalyst particles [11]. The formation of thin CNT is characteristic of Mo-including catalysts. Figures 1 (c) and (d) show CNT produced at 823 K by $\text{Co}_{0.2}\text{Mg}_{0.8}\text{O}$ and $\text{Co}_{0.3}\text{Mg}_{0.7}\text{O}$ catalysts, respectively. The outer diameters ranged from 7 to 27 nm, and no CNTs of thin outer diameter were observed. The Mo-free Co catalysts thus produce thicker CNT by decomposition of CH_4 .

The crystallinity of CNT was evaluated by Raman spectroscopy. Figure 2 shows the Raman spectra of CNT obtained at 1073 K for 1 h using Mo/Co/MgO and Co/MgO catalysts with different mole fractions. All of these spectra show two broad bands at 1360 cm^{-1} (D-band) and 1582 cm^{-1}

(G-band). The D-band is associated with the vibrations of carbon atoms with dangling bonds in plane terminations of "disordered graphite" (i.e., turbostratic carbon) or glassy carbons. The G-band corresponds to the E_{2g} mode of graphite, and is related to the vibration of sp^2 -bonded carbon atoms in the two dimensional hexagonal lattice of the graphite layer. In general, the G-band represents the degree of crystallinity in the graphite structure, while the intensity of the D-band indicates the defects, impurities or lattice distortions in the carbon nanotubes. The I_G/I_D intensity ratio for CNT synthesized over Co/MgO was 1.5-1.7 independent of the composition and was larger than those over Mo/Co/MgO catalysts. That is, the crystallinity of CNT synthesized using Co/MgO is better than that synthesized using Mo/Co/MgO. This is ascribed to thicker graphene layers of CNT produced over Co/MgO. The I_G/I_D intensity ratio of 0.8-1.0 for Mo/Co/MgO was comparable with those for Mo/Ni/MgO (0.8-1.0 at 1073 K for 1 h)[11]. That is, the quality of CNT synthesized using Mo/Co/MgO catalysts is similar to that synthesized using Mo/Ni/MgO catalysts.

To examine the effect of Mo in Mo/Co/MgO catalysts, the kinetics of the CNT formation from CH_4 were compared for Mo/Co/MgO and Co/MgO catalysts. Figure 3 shows the carbon or CNT yield produced using $Mo_{0.1}Co_{0.4}Mg_{0.5}O$, $Mo_{0.4}Co_{0.1}Mg_{0.5}O$, and $Co_{0.5}Mg_{0.5}O$ catalysts for 1 h by decomposition at 37.5 Torr CH_4 as a function of the reaction temperature. At the lower reaction temperatures, below 923 K, yields for the Co/MgO catalyst were higher than those for the Mo/Co/MgO catalyst. On the other hand, the carbon yield at higher temperatures, above 923 K, significantly increased over the Mo/Co/MgO catalysts, while it decreased over the Co/MgO catalysts. The catalytic activity of Mo/MgO was also measured as shown in Fig.3. The carbon yield was very low at temperatures below 1100 K, suggesting little catalytic activity of Mo (or Mo_2C) for CH_4 decomposition. The catalyst component of Co (or Ni or Fe) is necessary for the synthesis of CNT by CH_4 decomposition at lower temperatures below 1000 K.

The significant effects on catalytic activity of the addition of Mo to Co/MgO were examined by setting two temperature regimes, i.e., one above and one below 923 K. In the higher temperature regime, the decrease in the carbon yield over Co/MgO would be due to the deactivation of the Co

catalyst by carbon deposits. To examine this possibility, the carbon yield as a function of reaction time was measured over the Co/MgO catalyst at a lower, (823 K) and a higher (973 K) temperature, as shown in Fig. 4. At 823 K, some deactivation of catalyst was observed, while the Co/MgO catalyst was deactivated significantly at 973 K and lost catalytic activity within 3 h. The deactivation means that no decomposition of CH₄ takes place on the catalyst surface, which is ascribed to carbon deposition on the surface of the Co catalyst.

The deactivation of the Co/MgO catalysts by carbon deposits would be controlled by the kinetic balance of the following elementary steps: i) CH₄ decomposition into carbon and hydrogen, ii) carbon dissolution into Co bulk, iii) the segregation of carbon from the bulk to the surface of Co, and iv) the formation of a graphene network. At temperatures higher than 923 K, the decomposition rate of CH₄ on Co catalyst particles should increase significantly because the CH₄ decomposition is usually an activation process [12]. Also, the segregation rate of carbon from the bulk of Co will be greater than that of the carbon dissolution because the decomposition of Co₂C is thermodynamically favored at 700 K [13, 14, 15]. The increases in the rates of both CH₄ decomposition and carbon segregation will lead to an increase in the rate of carbon accumulation at the Co surface. That is, the rate of graphene formation is unable to match that of the accumulation of carbon.

Deactivation was also examined on a Mo/Co/MgO catalyst at the high temperature of 1073 K, as shown in Fig. 5. It was found that the catalytic activity was retained even at 8 h without deactivation. This is basically the same characteristic observed for the results of Mo/Ni/MgO catalysts [11]. It is considered that the length of the CNT increased with reaction time, with the number and the diameter of CNT being kept constant. The absence of deactivation for Mo/Co/MgO catalysts at high temperatures is a point of difference with Co/MgO catalysts, which is due to the kinetic balance of the elementary carbon-related steps. We thus carried out kinetic measurements as described in the next sections.

3.2 Pressure dependence

The dependence of CH₄ pressure upon the rate of CNT synthesis was examined for Co/MgO and Mo/Co/MgO catalysts to ascertain the rate-determining step. Figure 6 shows the carbon yield on a Co_{0.4}Mg_{0.6}O catalyst at 823 K as a function of reaction time at various CH₄ pressures. The initial reaction rate for carbon deposition can be obtained from the slope at t=0. The rate was thus evaluated as carbon yield (wt%) per hour. Here, gradual deactivation of catalyst can be recognized from a decrease in the slope. In Fig. 7, the slope was plotted against CH₄ pressure to obtain the reaction order, *n*, of CH₄ in the following reaction equation.

$$r = kP_{\text{CH}_4}^n \quad (1)$$

$$\text{or} \quad \ln r = \ln k + n \ln P_{\text{CH}_4}$$

The logarithmic plot of Fig. 7 clearly shows that the reaction order is unity, indicating that the dissociation of CH₄ on Co surface is the rate-determining step.

The reaction order was also examined for Mo/Co/MgO catalysts. Figure 8 shows the carbon yield on Mo_{0.1}Co_{0.4}Mg_{0.5}O at 1073 K as a function of reaction times at various CH₄ pressures. Even at high CH₄ pressures, no significant deactivation was observed. The logarithm of the initial slope was plotted against $\ln P_{\text{CH}_4}$ as shown in Fig. 9. Again, it was found that the reaction order, *n*, is equal to unity, indicating that the dissociation of CH₄ is the rate-determining step even at the high temperature of 1073 K. The results shown in Figs. 7 and 9 indicate that the rate-determining step is the dissociation of CH₄ if the catalyst is working without significant deactivation. In other words, the segregation of carbon or the assembling of carbon into graphene sheet is fast enough compared to the CH₄ dissociation. Otherwise, the surface carbon will be converted to the other forms of carbon, which then block the catalyst surface for CH₄ dissociation. The deactivation observed for Co/MgO at higher temperatures can thus be attributed to significant CH₄ dissociation compared to the rate of the graphene sheet assembly.

3.3 Temperature dependence

Figure 10 shows the Arrhenius plot for carbon deposition on Mo/Co/MgO and Co/MgO catalysts at 37.5 Torr CH₄. From the slopes, the apparent activation energies were estimated to be

150-163 kJ/mol and 96 kJ/mol for Mo/Co/MgO and Co/MgO catalysts, respectively. Since CH₄ dissociation is the rate-determining step, the activation energy may be comparable to that for CH₄ dissociation on a Co surface. The activation energy on Co/MgO seems to be higher than literature data of CH₄ decomposition (66.3 kJ/mol) [16].

As shown in Fig.3, the addition of Mo into Co/MgO catalysts reduced the reaction rate of CH₄ dissociation at 773-923 K. This is consistent with the increase of the activation energy of CH₄ dissociation. The reduction in the catalytic activity of Mo/Co/MgO for the CH₄ dissociation would be related to the uniqueness of the catalyst for producing thin CNT at high reaction temperatures as described in section 3.5.

3.4 XRD measurements

To examine the state of the catalysts, XRD measurements were carried out for Co/MgO and Mo/Co/MgO catalysts after reduction with H₂ and after CNT synthesis. Figures 11 and 12 show XRD patterns for Co/MgO and Mo/Co/MgO catalysts, respectively. For the Co/MgO catalyst after calcinations, the peaks assigned to Co₃O₄ at $2\theta=19.05^\circ$, 31.24° , 44.75° , 59.37° , and 65.21° were observed in addition to MgO peaks [17, 18]. After reduction with H₂, a new peak attributed to metallic Co appeared at $2\theta=44.16^\circ$ and 51.36° , which did not change after CNT synthesis [19]. On the other hand, the Mo/Co/MgO catalyst after calcinations shows the presence of mixed oxides of MgMoO₄ and CoMoO₄ [17, 20]. After reduction of the mixed oxides, new peaks appeared at $2\theta=40.23^\circ$ and 45.19° indicating the formation of Mo-rich Mo-Co alloys [21]. This further suggests that Mo and Co are present in catalyst particles. The coexistence of Mo and Co in the Mo/Co/MgO catalysts is similar to that of Mo and Ni in the Mo/Ni/MgO catalysts [11]. After CNT synthesis new peaks attributed to Mo₂C appeared at $2\theta=39.53^\circ$ [22, 23]. So it is considered that carbon was mixed into metallic Mo, and then Mo transformed into a stable species, Mo₂C, during CNT synthesis.

3.5 Role of catalyst component

This study shows that the rate-determining step is the CH₄ decomposition for continuous synthesis of CNT in order to keep catalysts active for CNT synthesis. If the rate of CH₄ dissociation

exceeds that of the formation of the graphene network, carbon species such as amorphous carbon will accumulate and cover the catalyst surface, leading to the deactivation of the CH_4 decomposition. Concerning the kinetic balance in the CNT synthesis, two significant effects of Mo in the Mo/Co/MgO catalyst were observed. First, the addition of Mo into Co/MgO decreased the catalytic activity for the dissociation of CH_4 as described in 3.3. Here, the rate-determining step of the CNT synthesis was the CH_4 dissociation. Second, molybdenum carbide was formed during CNT synthesis. The two effects mean that at higher temperatures CH_4 dissociation is relatively slow compared to the segregation of carbon to the bulk and the formation of a graphene network, which is the reason why the Mo/Co/MgO catalysts work at high temperatures without carbon deactivation. The formation of Mo_2C in the catalyst particles plays a role in preserving carbon in the catalyst particle.

Another possible effect of Mo is the production of thin CNT with good quality. The presence of the stable Mo_2C will prevent the fluctuation in the shape of catalyst particles during CNT synthesis at the high temperature of 1073 K. As has been reported by video of *in situ* TEM measurements, because of thermal fluctuation the shape of a Ni catalyst particle frequently changes at 773-813 K during CNT synthesis [24]. Probably, the fluctuation leads to low quality in the crystallinity of CNT. On the other hand, Mo_2C is known to be a very hard material with a high decomposition temperature of 1273 K [11]. The thermal stability of Mo_2C will help stably grow CNT with good crystallinity at high temperatures.

It should be noted that the coexistence of Co and Mo_2C in a single catalyst particle is important for its operation as a bi-functional catalysts. The Co component is necessary for the dissociation of CH_4 . The mixture of Co and Mo in the single particle is successfully realized by forming the Mo-Co alloy in the reduction procedure of the catalyst preparation. The Mo-Co alloy phase will change to Mo_2C and Co phases during CNT synthesis. This is similar to the case of Mo/Ni/MgO catalysts [11]. Finally, the role of MgO is to disperse Mo and Co as small metal particles, which initially are mixed together by forming mixed metal oxides.

4. Conclusion

Thin CNTs of 3-10 nm outer diameters were formed by decomposition of CH_4 over Mo/Co/MgO catalysts at temperatures higher than 923 K. Whereas, thick CNTs were produced over Co/MgO catalysts at the lower reaction temperatures of 823-923 K. Mo/Co/MgO catalysts were active at higher temperatures above 923 K, but Co/MgO catalysts were deactivated by carbon deposition. The absence of deactivation for Mo/Co/MgO catalysts is due to the kinetic balance of the carbon-related elementary steps. The rate-determining step would be that of CH_4 decomposition for continuous synthesis of CNT so as to keep catalysts active for CNT synthesis. Otherwise, surface carbon will be converted to the other forms of carbon that will block the catalyst surface for CH_4 dissociation. The deactivation observed for Co/MgO at higher temperatures is thus attributed to significant CH_4 dissociation compared to the rate of the graphene sheet formation. The role of Mo is; i) to reduce the dissociation activity of CH_4 , and ii) to keep carbide (Mo_2C) stable at high temperatures, which is why Mo/Co/MgO catalysts work at high temperatures without carbon deactivation.

References

- [1] Iijima S. Helical microtubules of graphitic carbon. *Nature* 1991; 354: 56-8.
- [2] Ebbesen TW, Ajayan PM. Large-scale synthesis of carbon nanotubes. *Nature* 1992; 358: 220-2.
- [3] Thess A, Lee R, Dai P, Petit P, Robert J, Xu C, et al. Crystalline ropes of metallic carbon nanotubes. *Science* 1996; 273: 483-7.
- [4] Hornyak GL, Dillon AC, Parilla PA, Schneider JJ, Czap N, Jones K, et al. Template synthesis of carbon nanotubes. *Nano Mater* 1999; 12: 83-8.
- [5] Rana RK, Koltypin Y, Gedanken A. Synthesis of carbon nanotubes from in situ generated cobalt nanoparticles and carbon monoxide. *Chem Phys Lett* 2001; 344: 256-62.
- [6] Thostenson ET, Ren Z, Chou TW. Advances in the science and technology of carbon nanotubes and their composites: a review. *Comp Sci Tech* 2001; 61: 1899-912.
- [7] Hafner JH, Bronikowski MJ, Azamian BR, Nikolaev P, Rinzler AG, Colbert DT, et al. Catalytic growth of single-wall carbon nanotubes from metal particles. *Chem Phys Lett* 1998; 296: 195-202.
- [8] Tang S, Zhong Z, Xiong Z, Liu L, Lin J, Shen ZX, et al. Controlled growth of single-walled carbon nanotubes by catalytic decomposition of CH₄ over Mo/Co/MgO catalysts. *Chem Phys Lett* 2001; 350: 19-26.
- [9] Hu MH, Murakami Y, Ogura M, Maruyama S, Okubo T. Morphology and chemical state of Co–Mo catalysts for growth of single-walled carbon nanotubes vertically aligned on quartz substrates. *J Catal* 2004; 225: 230-9.
- [10] Herrera JE, Balzano L, Borgna A, Alvarez WE, Resasco DE. Relationship between the structure/composition of Co–Mo catalysts and their ability to produce single-walled carbon nanotubes by CO disproportionation. *J Catal* 2001; 204: 129-45.
- [11] Zhou LP, Ohta K, Kuroda K, Ni L, Matsuishi K, Gao LZ, et al. Catalytic functions of Mo/Ni/MgO in the synthesis of Thin carbon nanotubes. *J Phys Chem B* 2005; 109: 4439-47.

- [12] Egeberg RC, Ullmann S, Alstrup I, Mullins CB, Chorkendorff I. Dissociation of CH₄ on Ni(1 1 1) and Ru(0 0 1). *Surf Sci* 2002; 497: 183-93.
- [13] Nagakura S. Study of metallic carbides by electron diffraction part iv. cobalt carbides. *J Phys Soc Japan* 1961; 16: 1213-9.
- [14] Hofer LJE, Peebles WC. Preparation and X-Ray diffraction studies of a new cobalt carbide. *J Am Chem Soc* 1947; 69: 893-9.
- [15] Nakamura J, Toyoshima I, Tanaka K. Formation of carbidic and graphitic carbon from CO on polycrystalline cobalt. *Surf Sci* 1988; 201: 185-94.
- [16] Zhang Y, Smith KJ. CH₄ decomposition on Co catalysts: effect of temperature, dispersion, and the presence of H₂ or CO in the feed. *Catal Today* 2002; 77: 257-68.
- [17] Radwan NRE, Ghosza AM, El-Shobaky GA. Solid–solid interactions in Co₃O₄–MoO₃/MgO system. *Therm Acta* 2003; 398: 211-21.
- [18] Radwan Nagi RE, El-Shobaky GA, Fahmy YM. Cordierite as catalyst support for cobalt and manganese oxides in oxidation–reduction reactions. *Appl Catal A: General* 2004; 274, 87-99.
- [19] Martin M, Koops U, Lakshmi N. Reactivity of solids studied by in situ XAS and XRD. *Sol State Ion* 2004; 172: 357-63.
- [20] Fazle Kibria AKM, Shajahan Md, Mo YH, Kim MJ, Nahm KS. Long activity of Co–Mo/MgO catalyst for the synthesis of carbon nanotubes in large-scale and application feasibility of the grown tubes. *Diam Rel Mater* 2004; 13: 1865-72.
- [21] Lee CR, Kang SG. Electrochemical stability of Co–Mo intermetallic compound electrodes for hydrogen oxidation reaction in hot KOH solution. *J Power Sour* 2000; 87: 64-8.
- [22] Claridge JB, York APE, Brungs AJ, Alvarez CM, Sloan J, Tsang SC, et al. New catalysts for the conversion of methane to synthesis gas: molybdenum and tungsten carbide. *J Catal* 1998; 180: 85-100.
- [23] Xiao T, Wang H, Da J, Coleman KS, Green MLH. Study of the preparation and catalytic performance of molybdenum carbide catalysts prepared with C₂H₂/H₂ carburizing mixture. *J*

Catal 2002; 211: 183-91.

- [24] Helveg S, López-Cartes C, Sehested J, Hansen PL, Clausen BS, Rostrup-Nielsen JR, et al.
Atomic-scale imaging of carbon nanofibre growth. Nature 2004; 427: 426-9.

FIGURE CAPTIONS

Figure 1 TEM images of as-grown carbon nanotubes produced from catalytic decomposition of CH_4 : (a) and (b) at 1073 K for 8 h over $\text{Mo}_{0.025}\text{Co}_{0.05}\text{Mg}_{0.925}\text{O}$, (c) at 823 K for 3 h over $\text{Co}_{0.2}\text{Mg}_{0.8}\text{O}$, and (d) at 823 K for 3 h over $\text{Co}_{0.3}\text{Mg}_{0.7}\text{O}$. $P_{\text{CH}_4}=37.5$ Torr.

Figure 2 Raman spectra of carbon nanotubes produced at 923 K for 1 h over Mo/Co/MgO and Co/MgO catalysts with different mole fraction.

Figure 3 Relationship between reaction temperature and carbon yield (or CNT yield) on Mo/Co/MgO catalysts for 1 h: (\circ) $\text{Mo}_{0.1}\text{Co}_{0.4}\text{Mg}_{0.5}\text{O}$, (\times) $\text{Mo}_{0.4}\text{Co}_{0.1}\text{Mg}_{0.5}\text{O}$, (\blacksquare) $\text{Co}_{0.5}\text{Mg}_{0.5}\text{O}$. $P_{\text{CH}_4}=37.5$ Torr, (\blacktriangle) $\text{Mo}_{0.1}\text{Mg}_{0.9}\text{O}$ and ($+$) $\text{Mo}_{0.05}\text{Mg}_{0.95}\text{O}$.

Figure 4 Relationship between reaction time and carbon yield on $\text{Co}_{0.4}\text{Mg}_{0.6}\text{O}$ catalyst: (\bullet) 823 K and (\blacksquare) 973 K. $P_{\text{CH}_4}=37.5$ Torr.

Figure 5 Relationship between reaction time and carbon yield on $\text{Mo}_{0.025}\text{Co}_{0.05}\text{Mg}_{0.925}\text{O}$ catalyst at 1073 K. $P_{\text{CH}_4}=37.5$ Torr.

Figure 6 Carbon yield on $\text{Co}_{0.4}\text{Mg}_{0.6}\text{O}$ at 823 K as a function of reaction times at various CH_4 pressures: (\triangle) 78.0 Torr, (\blacktriangle) 37.5 Torr, (\times) 22.5 Torr and (\bullet) 7.5 Torr.

Figure 7 Logarithm plot of CH_4 pressure and the initial reaction rate for carbon deposition on $\text{Co}_{0.4}\text{Mg}_{0.6}\text{O}$ catalyst at 823 K.

Figure 8 Carbon yield on $\text{Mo}_{0.1}\text{Co}_{0.4}\text{Mg}_{0.5}\text{O}$ at 1073 K as a function of reaction times at various CH_4 pressures: (\triangle) 78.0 Torr, (\blacktriangle) 37.5 Torr, (\times) 22.5 Torr and (\bullet) 7.5 Torr.

Figure 9 The logarithm plot of CH_4 pressure and the initial reaction rate for the carbon deposition on $\text{Mo}_{0.1}\text{Co}_{0.4}\text{Mg}_{0.5}\text{O}$ catalyst at 1073 K.

Figure 10 The Arrhenius plot of the carbon yield on Mo/Co/MgO catalyst: (\circ) $\text{Mo}_{0.1}\text{Co}_{0.4}\text{Mg}_{0.5}\text{O}$, (\times) $\text{Mo}_{0.4}\text{Co}_{0.1}\text{Mg}_{0.5}\text{O}$ and (\blacksquare) $\text{Co}_{0.5}\text{Mg}_{0.5}\text{O}$. $P_{\text{CH}_4}=37.5$ Torr.

Figure 11 XRD pattern of $\text{Co}_{0.4}\text{Mg}_{0.6}\text{O}$ catalyst after calcinations at 823 K and after reduction with H_2 at 923 K for 1 h and after CNT synthesis at 973 K for 1 h.

Figure 12 XRD pattern of $\text{Mo}_{0.1}\text{Co}_{0.4}\text{Mg}_{0.5}\text{O}$ catalyst after calcinations at 823 K, after reduction

with H₂ at 923 K for 1 h and after CNTynthesis at 1073 K for 1 h.

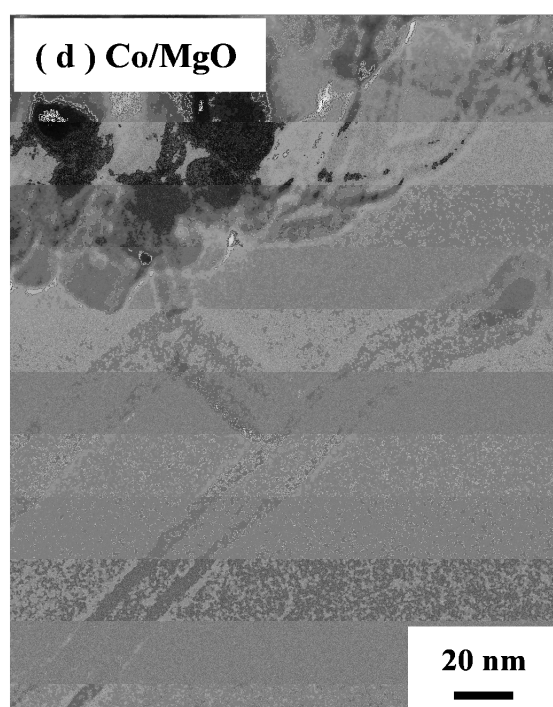
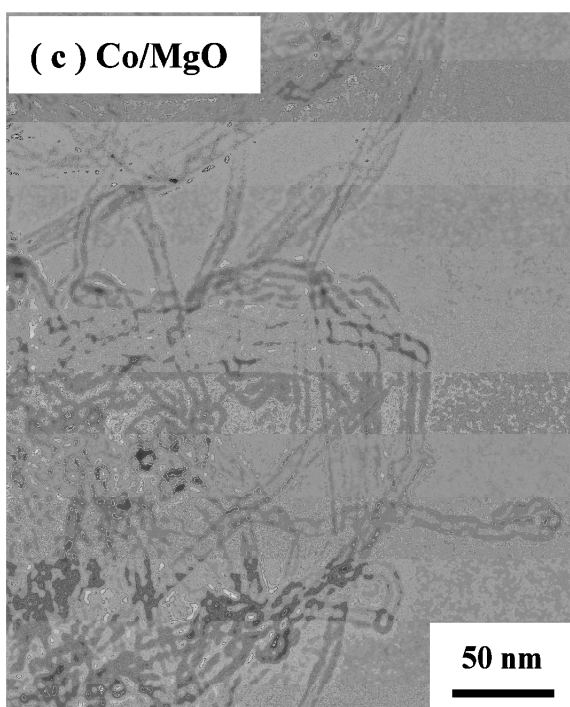
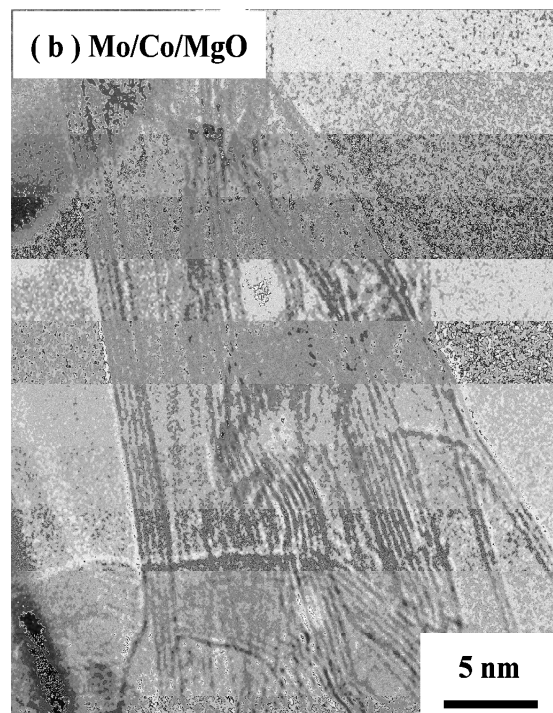
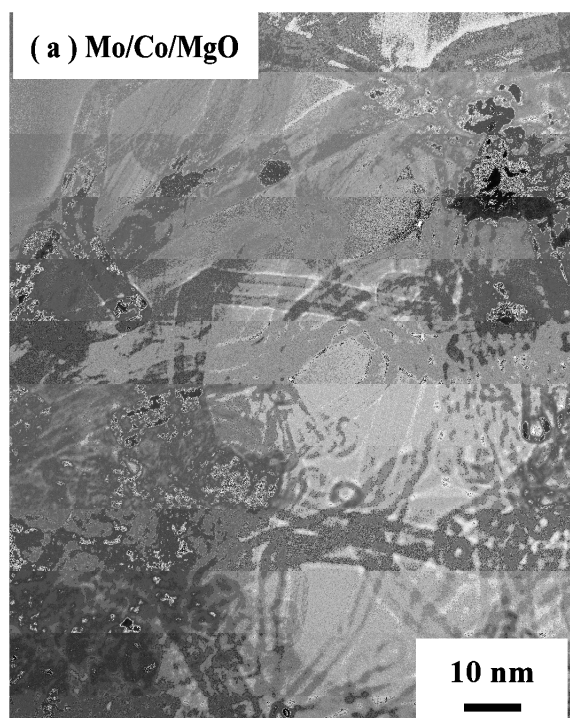


Fig. 1 L. Ni et al.

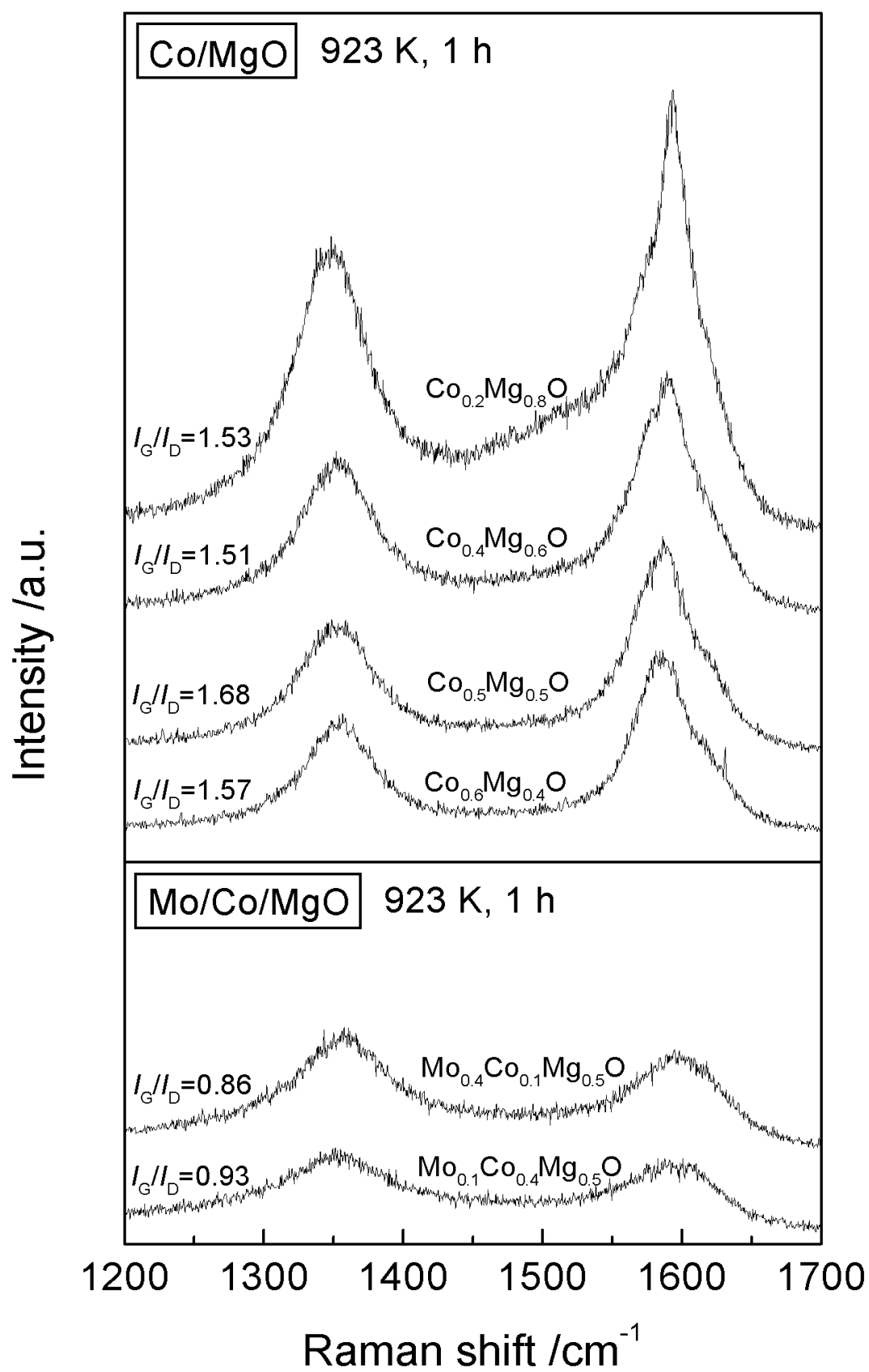


Fig. 2 L. Ni et al.

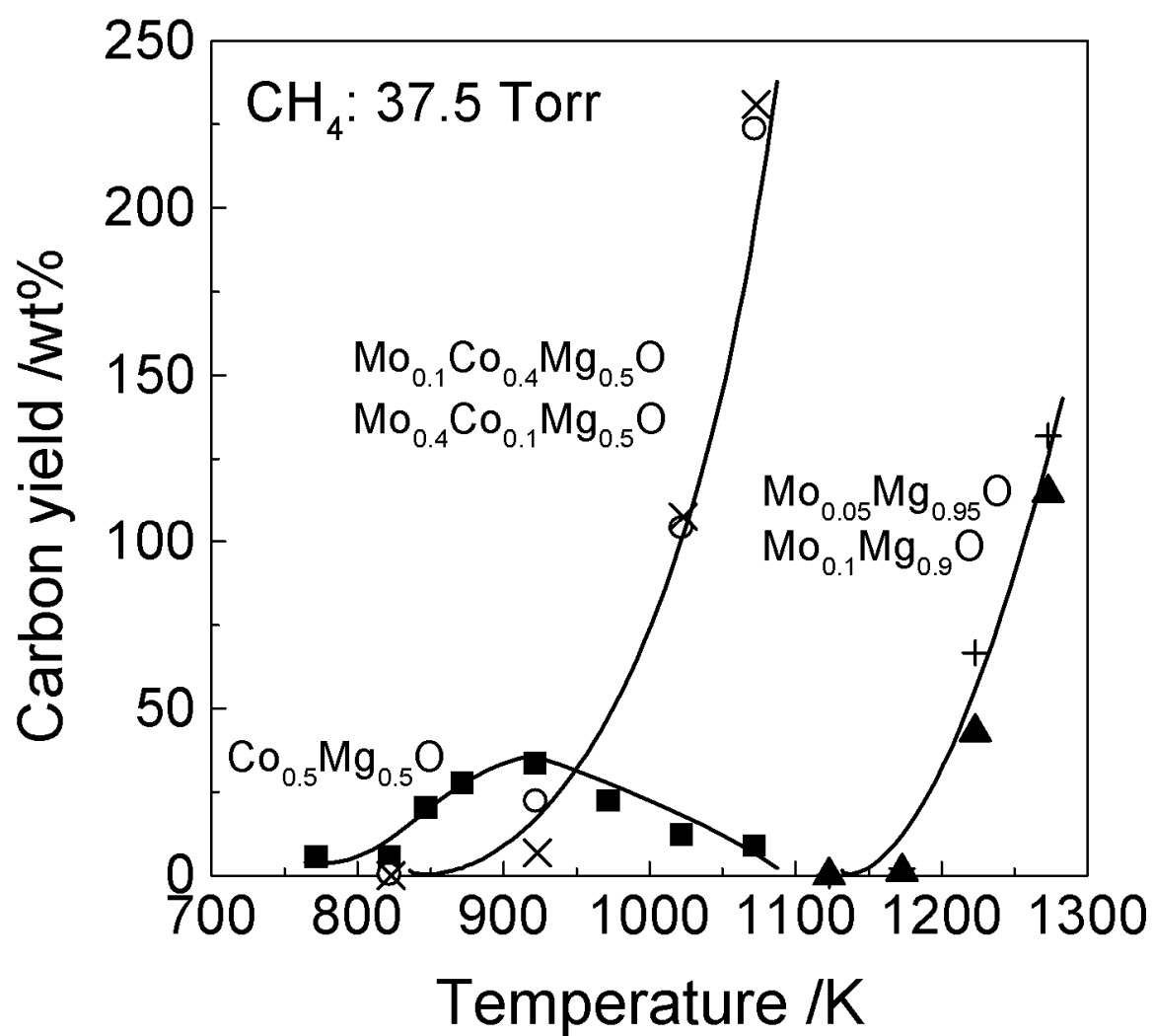


Fig. 3 L. Ni et al.

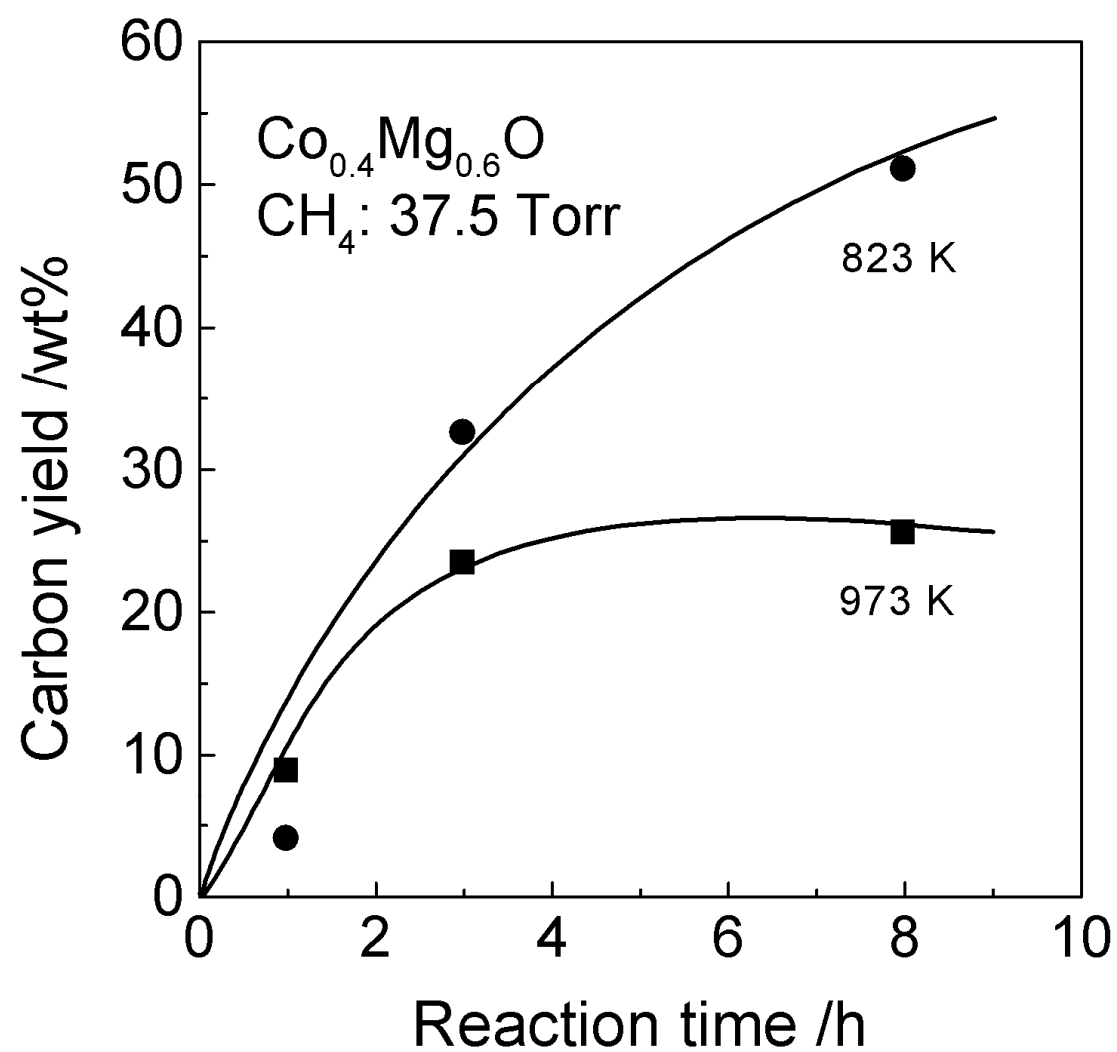


Fig. 4 L. Ni et al.

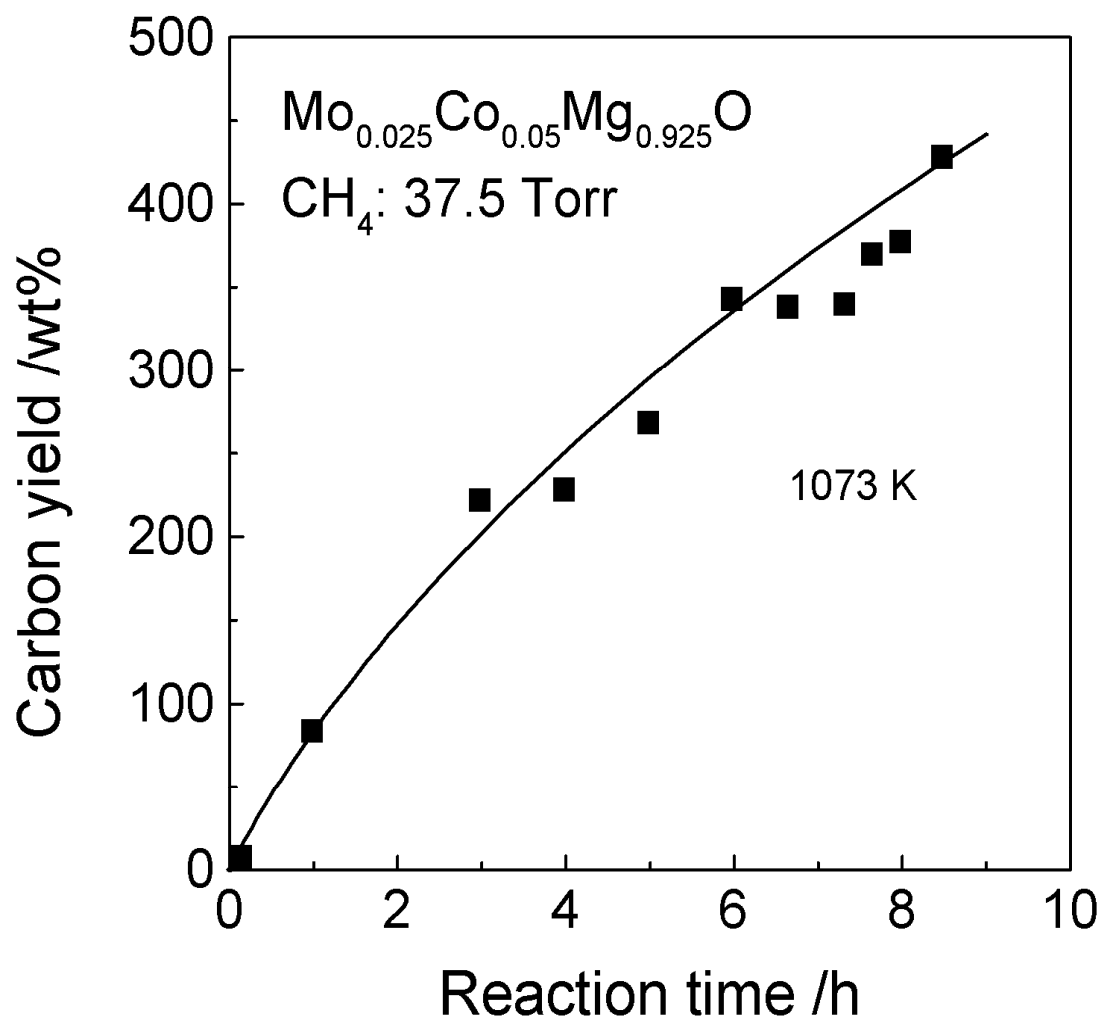


Fig. 5 L. Ni et al.

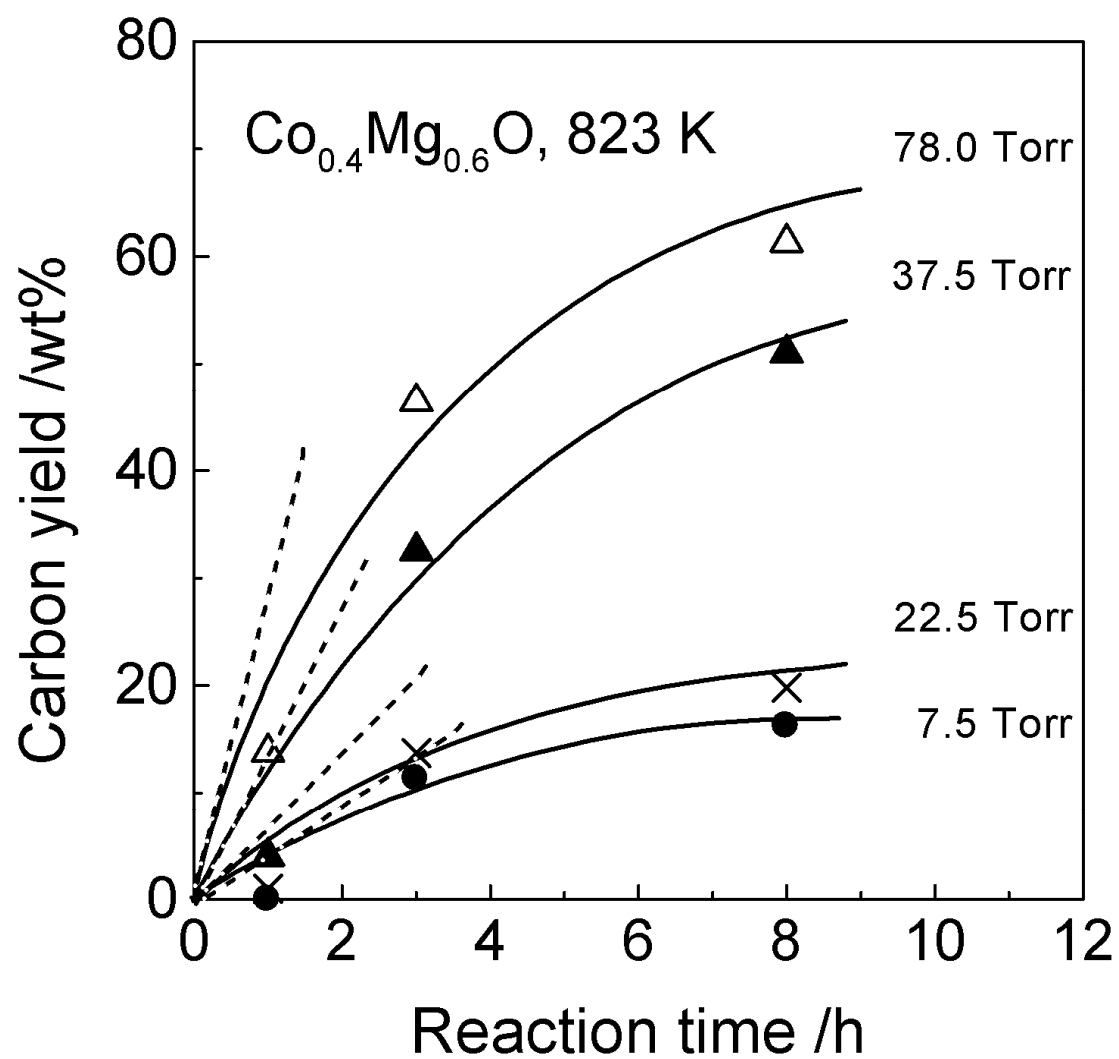


Fig. 6 L. Ni et al.

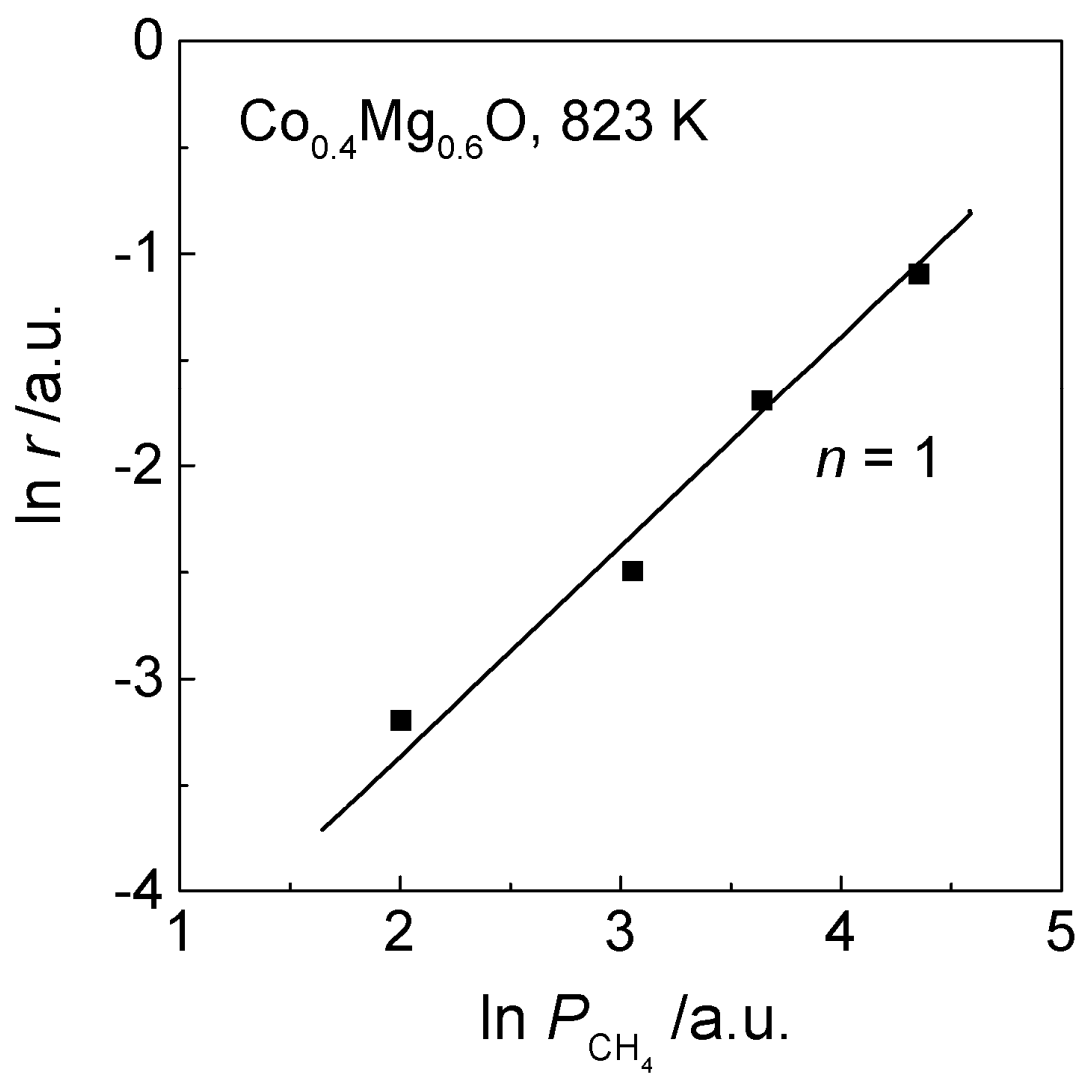


Fig. 7 L. Ni et al.

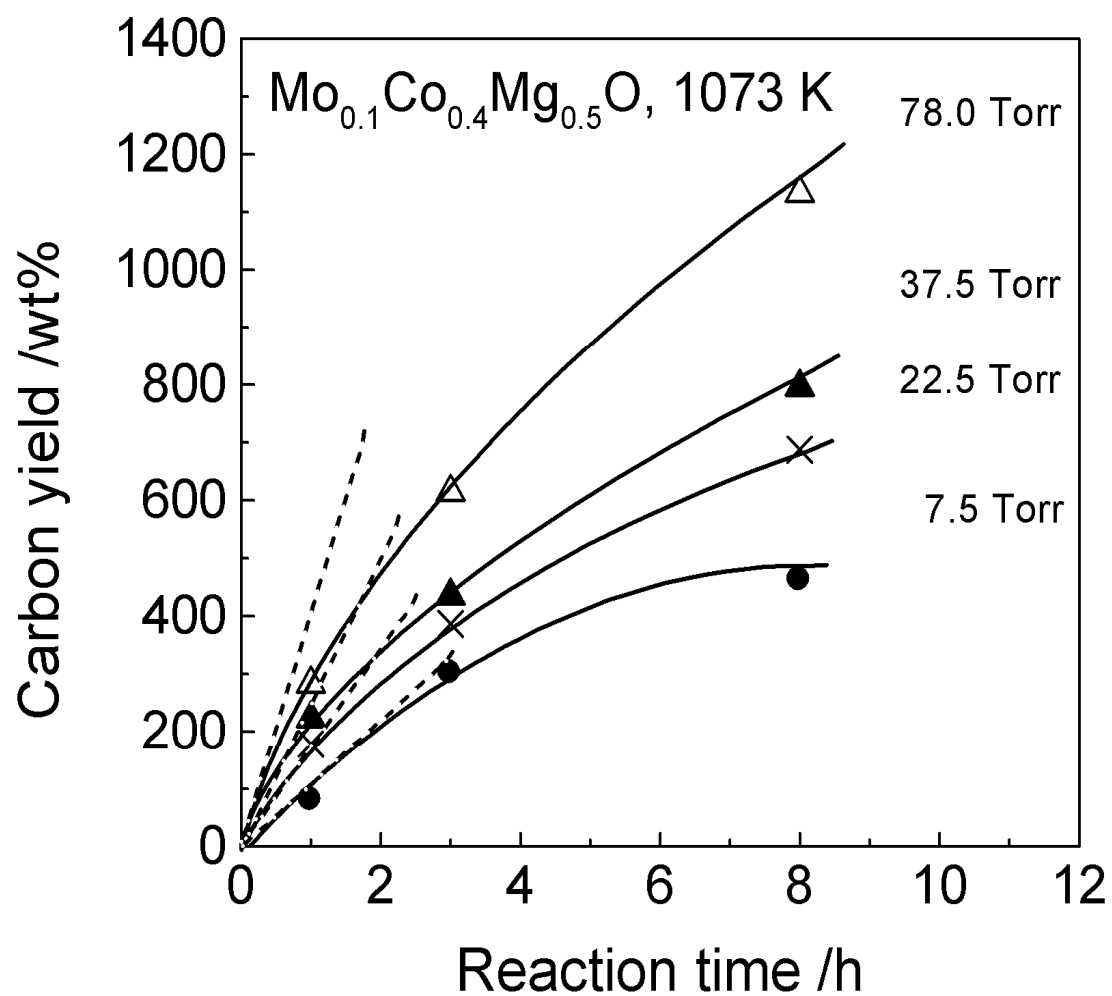


Fig. 8 L. Ni et al.

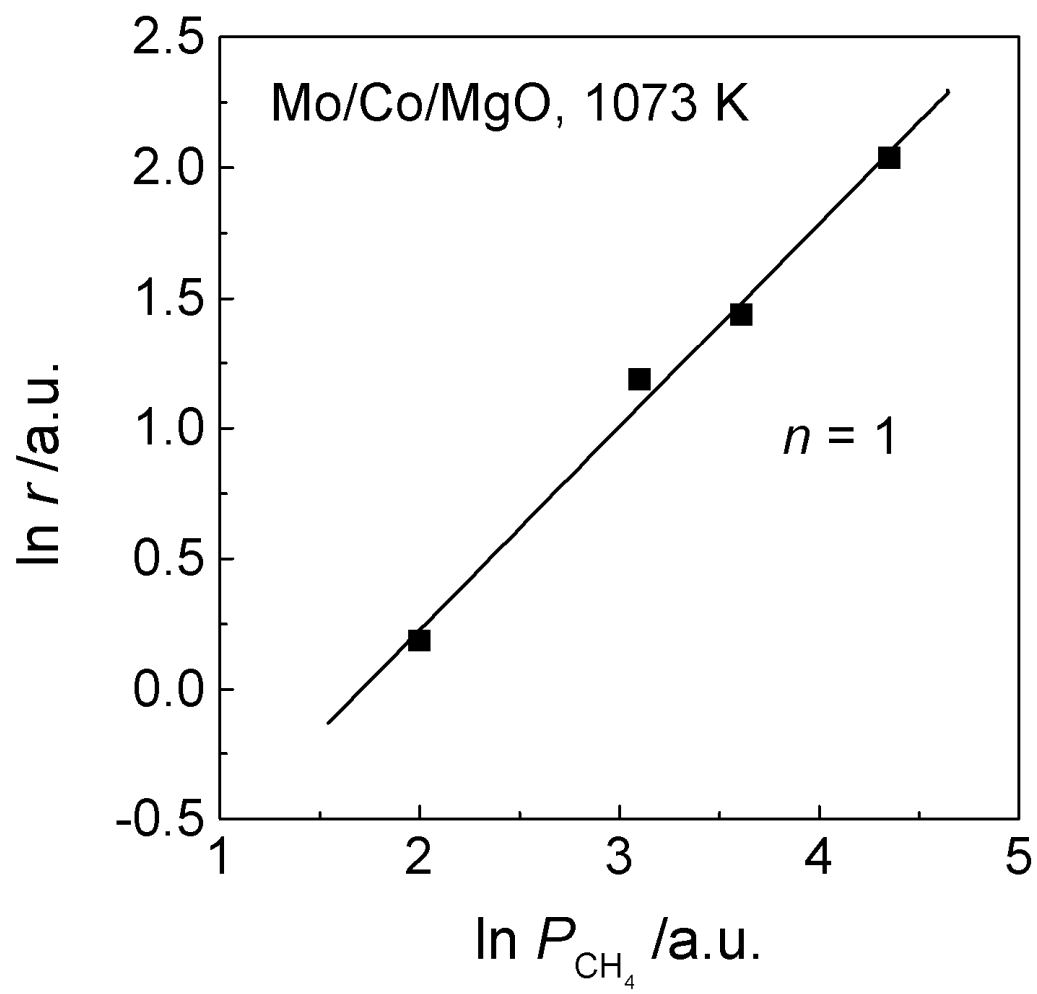


Fig. 9 L. Ni et al.

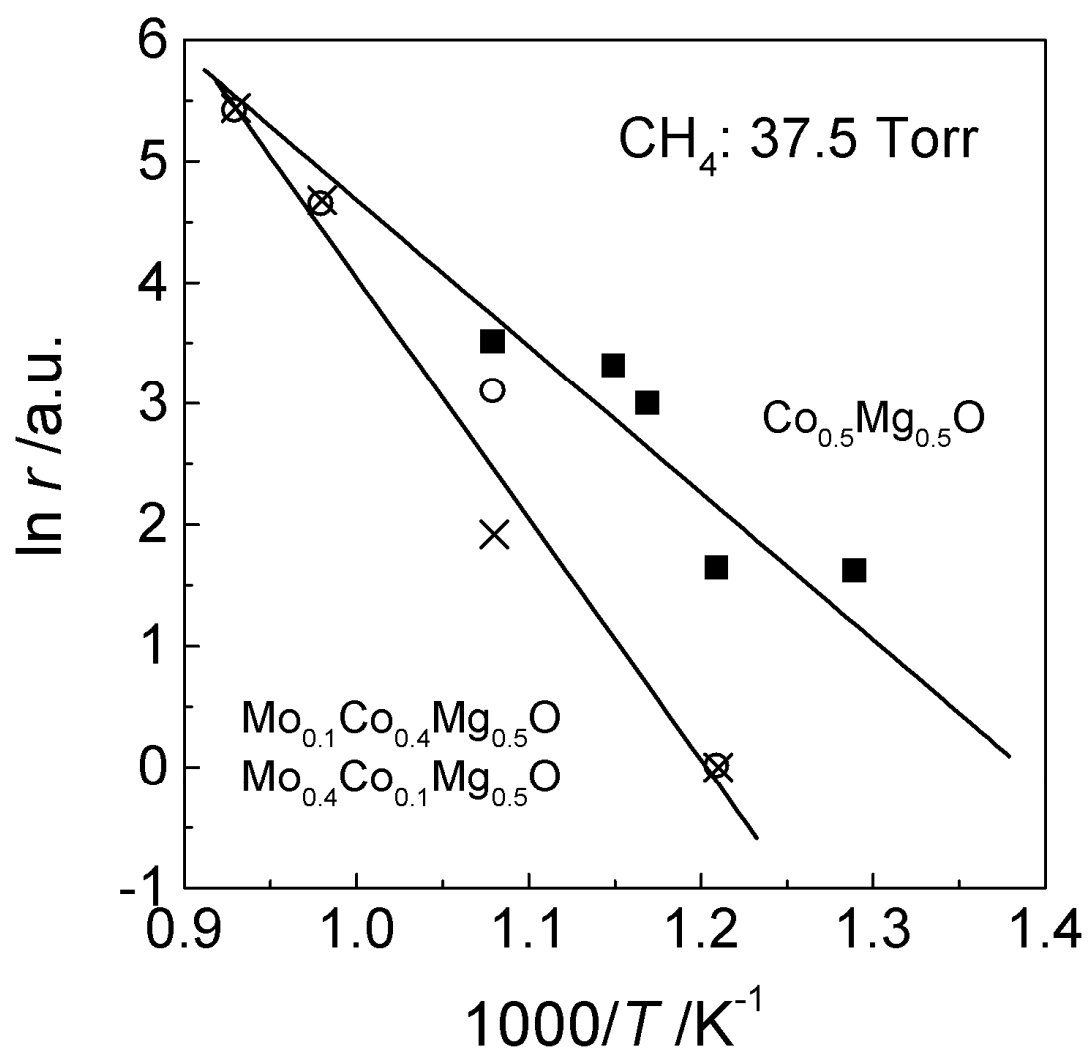


Fig. 10 L. Ni et al.

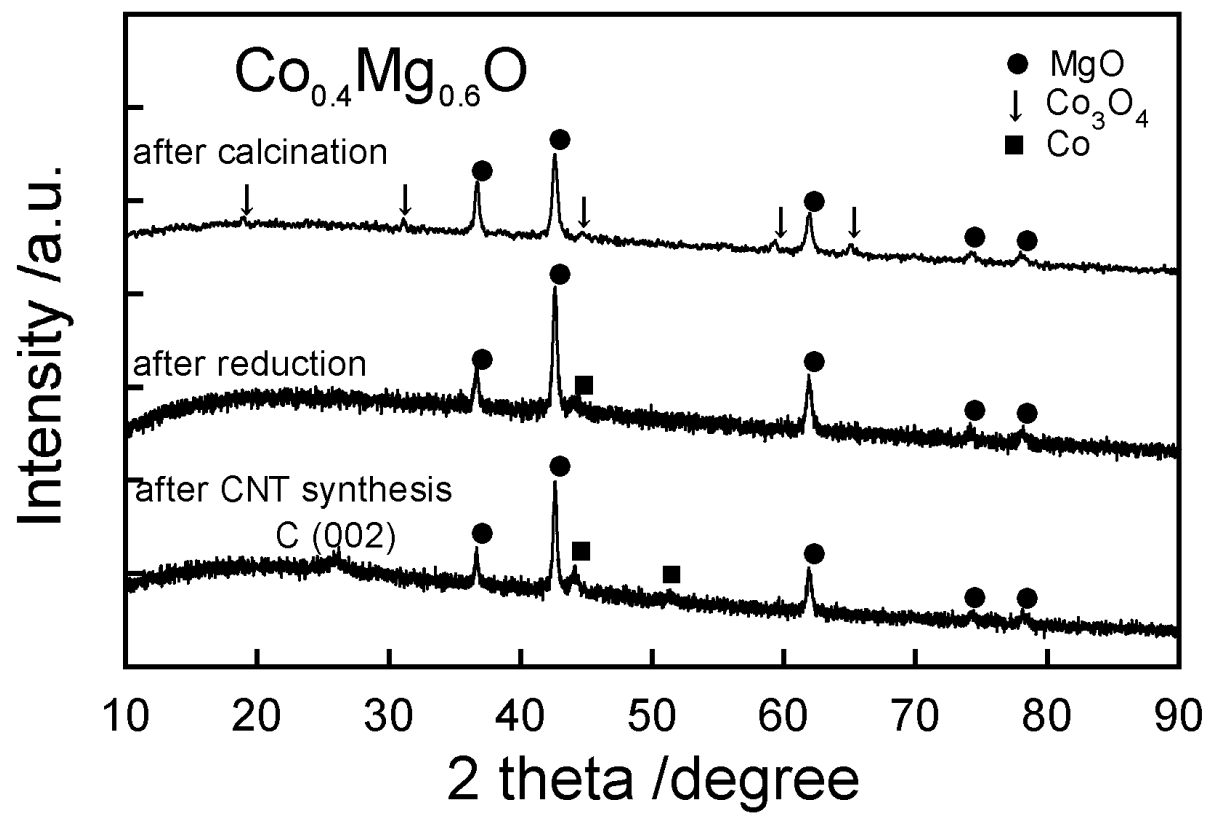


Fig. 11 L. Ni et al.

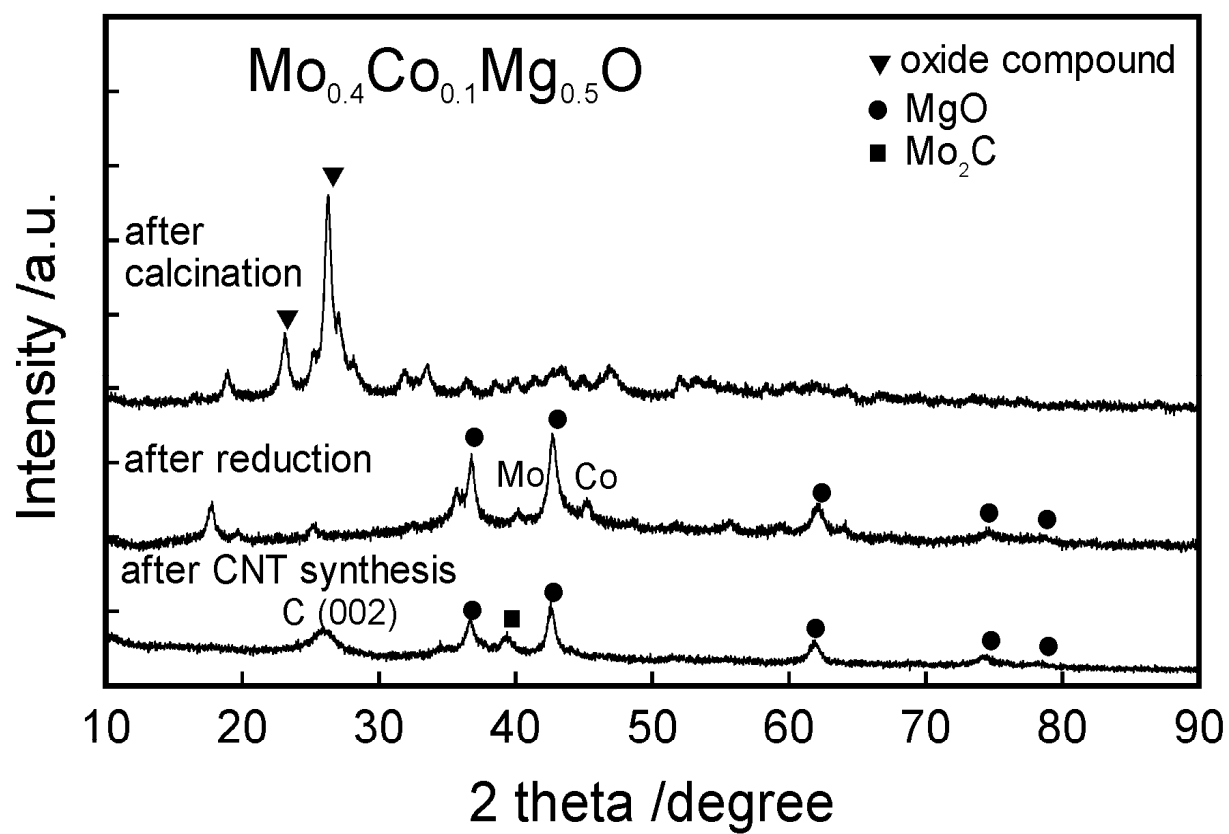


Fig. 12 L. Ni et al.